Biochemistry 1993, 32, 7712–7719

# Kinetic and Equilibrium Analysis of the Interactions of Actomyosin Subfragment-1·ADP with Beryllium Fluoride†

Brigitte C. Phan,*,‡ Larry D. Faller,§ and Emil Reisler*,‡

*Department of Chemistry and Biochemistry and Molecular Biology Institute, University of California, Los Angeles, California 90024, and Center for Ulcer Research and Education, Department of Medicine, University of California, Los Angeles School of Medicine, and Department of Veterans Affairs Medical Center West Los Angeles, Wadsworth Division, Los Angeles, California 90073*

*Received December 14, 1992; Revised Manuscript Received May 24, 1993*

ABSTRACT: The hypothesis that the stable ternary complex formed between myosin subfragment-1, MgADP and beryllium fluoride ($BeF_3^-$), denoted S-1$^{\neq}$·ADP·$BeF_3^-$, is an analog of the intermediate state S-1**·ADP·$P_i$ has been tested in this work by examining the interactions of S-1$^{\neq}$·ADP·$BeF_3^-$ with actin. Equilibrium binding measurements revealed that actin bound weakly to the S-1$^{\neq}$·ADP·$BeF_3^-$ complex ($K_a = 10^4\ M^{-1}$) in the presence of 40 mM KCl. The stability of this complex was strongly salt-dependent. The association constant of $BeF_3^-$ to the acto-S-1·ADP complex ($K_{Be} \sim 10^3\ M^{-1}$) was 100-fold weaker than its binding to the S-1·ADP complex. While inhibiting the S-1 ATPase strongly, $BeF_3^-$ had no effect on the $V_{max}$ value ($10 \pm 1.0\ s^{-1}$) of the actin-activated ATPase of S-1. The rates of $BeF_3^-$ binding and dissociation from the acto-S-1·ADP·$BeF_3^-$ complex were determined by stopped-flow measurements. The hyperbolic dependence of the rates of $BeF_3^-$ binding to acto-S-1·ADP ($k_{obs}$) on $BeF_3^-$ concentrations suggested that the acto-S-1·ADP·$BeF_3^-$ complex was formed in at least two steps: binding followed by isomerization. The binding constant was $1.2 \times 10^3\ M^{-1}$, and the maximum $k_{obs}$ was 2.5 $s^{-1}$. The dissociation of $BeF_3^-$ from the acto-S-1·ADP·$BeF_3^-$ complex was monitored via decrease in the fluorescence of 1-$N^6$-ethenoadenosine diphosphate (εADP). The fluorescence decrease fitted two exponential terms. A kinetic scheme which is consistent with earlier results on the interactions of S-1·ADP with $BeF_3^-$ (Phan & Reisler, 1992) and accounts for two exponential terms involves an equilibrium between two isomerized states S-1$^{\neq}$·ADP·$BeF_3^-$ and S-1$^{\neq\neq}$·ADP·$BeF_3^-$. The rate constant for the dissociation of $BeF_3^-$ from the S-1$^{\neq}$·ADP·$BeF_3^-$ complex was increased between $10^4$- and $10^5$-fold by actin. These results show that the AS-1$^{\neq}$·ADP·$BeF_3^-$ complex has properties similar to those of the intermediate state AS-1**·ADP·$P_i$ and thus support the hypothesis that S-1$^{\neq}$·ADP·$BeF_3^-$ is a good analog of the S-1**·ADP·$P_i$ state.

Force production in muscle results from the actin-accelerated hydrolysis of ATP by myosin. The elucidation of this basic energy transduction process requires the characterization of the intermediates associated with the myosin ATPase pathway. Analogs of ATP and phosphate which trap such intermediates are needed for this purpose.

Beryllium fluoride ($BeF_3^-$)[1] and aluminum fluoride ($AlF_4^-$) belong to a relatively new class of phosphate analogs which inhibit several ATPases including actin (Combeau & Carlier, 1988) and myosin (Robinson et al., 1986; Issartel et al., 1992; Maruta et al., 1992; Phan & Reisler, 1992; Werber et al., 1992). They have been shown to bind to the catalytic sites of F1-ATPase (Issartel et al., 1991), actin-ADP (Combeau & Carlier, 1988), and heavy meromyosin (Maruta et al., 1991) with a stoichiometry of 1:1. In the presence of ADP, $AlF_4^-$ and $BeF_3^-$ bind to the active site of myosin subfragment-1 (S-1), presumably with a 1:1 stoichiometry, and form stable ternary complexes, denoted M$^{\neq}$·ADP·$AlF_4^-$ and M$^{\neq}$·ADP·$BeF_3^-$, respectively (Maruta et al., 1991; Phan & Reisler, 1992; Werber et al., 1992, Beck et al., 1992). The formation of the complex M$^{\neq}$·ADP·$BeF_3^-$ has been shown to consist of at least two steps, a fast equilibrium binding followed by a slow isomerization step:

$$\mathrm{M{\cdot}ADP} + \mathrm{BeF_3^-} \overset{K_1}{\rightleftharpoons} \mathrm{M{\cdot}ADP{\cdot}BeF_3^-} \overset{K_2}{\rightleftharpoons} \mathrm{M^{\neq}{\cdot}ADP{\cdot}BeF_3^-}$$

The analogy between the M$^{\neq}$·ADP·$BeF_3^-$ complex and the predominant steady-state intermediate M**·ADP·$P_i$ of the $Mg^{2+}$-dependent ATPase pathway was suggested by kinetic measurements and a similar enhancement of the tryptophan fluorescence of myosin in both states (Phan & Reisler, 1992; Werber et al., 1992). In addition to this, a conformational analogy between the M$^{\neq}$·ADP·$BeF_3^-$ complex and the complex formed by myosin, ADP, and vanadate (M†·ADP·$V_i$) has been inferred from kinetic analysis of the inhibition of myosin ATPase and from experiments using εADP (Phan & Reisler, 1992). Since the complex M†·ADP·$V_i$ is considered, itself, to be an analog of the transition state M**·ADP·$P_i$ (Goody et al., 1980; Goodno, 1979; Wells & Bagshaw, 1984; Goodno & Taylor, 1982; Smith & Eisenberg, 1990), the similarities between the M$^{\neq}$·ADP·$BeF_3^-$ and the M$^+$·ADP·$V_i$ complexes provide additional support for the hypothesis that the M$^{\neq}$·ADP·$BeF_3^-$ complex is an analog of the M**·ADP·$P_i$ state.

The interaction of vanadate with myosin·ADP was also studied in the presence of actin (Goodno & Taylor, 1982;

† This work was supported by USPHS Grants AR22031 (E.R.) and DK36873 (L.D.F.), Atherosclerosis Training Grant HL 07386 (B.C.P.), Grants MCB 9206739 (E.R.) and MCB 9106338 (L.D.F.) from the National Science Foundation, and a VA Merit Review Award (L.D.F.).

* To whom correspondence should be addressed.

‡ Department of Chemistry and Biochemistry and Molecular Biology Institute.

§ UCLA School of Medicine and Department of Veterans Affairs Center West Los Angeles.

[1] Abbreviations: A, actin; M, myosin; S-1, myosin subfragment-1; $BeF_3^-$, beryllium fluoride, $AlF_4^-$, aluminum fluoride; $V_i$, vanadate; εADP, 1-$N^6$-ethenoadenosine diphosphate; ATPγS, adenosine 5'-O-(3-thiotriphosphate); PIPES, 1,4-piperazinediethanesulfonic acid.

0006-2960/93/0432-7712$04.00/0 

Smith & Eisenberg, 1990). However, detailed kinetic analysis of these interactions is greatly limited by the extensive polymerization of vanadate and by its photochemical modification of myosin. Therefore, understanding the interactions of alternative phosphate analogs with actomyosin would facilitate the characterization of the M**·ADP·$P_i$ state.

The goal of the present study has been to characterize the interactions of beryllium fluoride with actomyosin. We show that actin binds weakly to the $M^{\neq}$·ADP·$BeF_3^-$ complex and that $BeF_3^-$ binds weakly to the acto-S-1·ADP complex. $BeF_3^-$, while inhibiting strongly the myosin subfragment-1 ATPase, has little effect on the actin-activated ATPase activity of myosin subfragment-1 at high actin concentration. The rate of release of ADP and $BeF_3^-$ is greatly increased by actin, and the stability of the acto-S-1·ADP·$BeF_3^-$ complex is strongly salt-dependent. These results suggest that the $AM^{\neq}$·ADP·$BeF_3^-$ complex has the same properties as the AM**·ADP·$P_i$ complex.

## MATERIALS AND METHODS

*Reagents.* ADP, ATP, beryllium (dissolved in 1% HCl), aluminum, and fluoride were purchased from Sigma Chemical Co. (St. Louis, MO). 1,$N^6$-Ethenoadenosine diphosphate ($\epsilon$ADP) was obtained from Molecular Probes Inc. (Junction City, OR). ATP$\gamma$S was purchased from Boehringer Mannheim (Indianapolis, IN). Crystalline acrylamide was obtained from Bio-Rad (Richmond, CA). Millipore-filtered distilled water and analytical-grade reagents were used in all experiments. Note that beryllium is toxic and may be carcinogenic and should be handled carefully.

*Proteins.* Myosin from rabbit psoas muscle was prepared according to Godfrey and Harrington (1970). Subfragment-1 (S-1) was prepared by chymotryptic digestion of myosin as described by Weeds and Pope (1977). S-1 was not separated into isozymes and was used as a mixture of S-1(A1) and S-1(A2). Rabbit skeletal muscle actin was prepared in G-actin buffer (0.5 mM $\beta$-mercaptoethanol, 0.2 mM ATP, 0.2 mM $CaCl_2$, and 5 mM Tris, pH 7.6) by the procedure of Spudich and Watt (1971). G-actin was polymerized by the addition of 2 mM $MgCl_2$. Protein concentrations were determined spectrophotometrically by using the following extinction coefficients at 280 nm: S-1, $E^{1\%} = 7.5\ cm^{-1}$; actin, $E^{1\%} = 11.5\ cm^{-1}$.

*Airfuge Binding Experiments.* S-1 (0–10 $\mu$M) was preincubated with $MgCl_2$ (2 mM), ADP (1 mM), $BeCl_2$ (between 0 and 1000 $\mu$M), and NaF (5 mM) for 30 min at 22 °C prior to addition of F-actin (4 $\mu$M). The standard solvent contained 40 mM NaCl and 10 mM Tris, pH 7.6. The reaction mixture was incubated for 20 min and centrifuged at 140000g for 20 min at room temperature in a Beckman air-driven ultracentrifuge. The pelleted proteins were resolubilized in the original solvent. The supernatant and the resolubilized proteins were denatured and run on SDS–polyacrylamide (10%) gels (Laemli, 1970). Coomassie Blue R-stained protein bands were scanned with a Biomed Instrument (Fullerton, CA) scanning densitometer interfaced to a DTK computer. The densitometric traces of the scanned protein bands were analyzed to determine the molar ratios of S-1 bound to actin. Molar ratios of bound proteins were calculated by using molar stain ratios obtained from appropriate calibration gels. Scatchard plots for the binding of S-1 to actin were constructed by expressing the amount of S-1 bound to actin as a function of free S-1. The apparent binding constant ($K_{app}$) at each beryllium fluoride concentration was calculated from the slope of the Scatchard plot. These apparent binding constants were plotted against 1/[$BeF_3^-$] and the binding constants of actin to S-1·ADP·$BeF_3^-$ and of $BeF_3^-$ to acto-S-1·ADP were obtained from the $y$ intercept and the slope of the plot, respectively (Greene & Eisenberg, 1980).

*Measurements of Actin-Activated ATPase Activity of S-1.* Actin-activated ATPase activities of S-1 in the presence and absence of beryllium fluoride were determined under steady-state conditions by a colorimetric assay in a solvent containing 3 mM ATP, 3 mM $MgCl_2$, 40 mM KCl, and 10 mM Tris, pH 7.6, at 25 °C. S-1 (3 $\mu$M) was preincubated with ADP (1 mM), $BeCl_2$ (from 0 to 1000 $\mu$M) and NaF (5 mM) for 30 min at 25 °C. Actin (from 0 to 30 $\mu$M) was added to this S-1 mixture immediately before ATP addition. The linear range of ATPase activities versus time was established for different actin concentrations. The assays, initiated by the addition of ATP, were carried out under steady-state conditions and stopped by addition of 10% trichloroacetic acid. The reported ATPase activities are given in turnover terms, i.e., in micromoles of $P_i$ released per micromole of S-1 per second. These values were not corrected for the negligible activities of S-1 alone.

*Dissociation of Acto-S-1 Nucleotide Complexes as a Function of Salt Concentration.* The dissociation of acto-S-1 nucleotide complexes was monitored by following the light scattering changes in a Spex Fluorolog spectrophotometer (Spex Industries, Inc., Edison, NJ) at 325 nm. The light scattering signal from the complex formed between S-1 (2.5 $\mu$M), actin (15 $\mu$M), and $MgCl_2$ (2 mM) was measured in the presence of ADP (1 mM), ATP$\gamma$S (2 mM), and ADP (1 mM) and $BeF_3^-$ (500 $\mu$M). The standard solvent contained 5 mM KCl and 10 mM Tris, pH 7.6. The acto-S-1 nucleotide complexes were formed in the standard solvent and then titrated with increasing amounts of KCl. At each KCl concentration, the percentage of acto-S-1 complex that dissociated was quantified by taking 100% dissociation as the scattering signal change induced by 2 mM ATP in the presence of 200 mM KCl.

*Stopped-Flow Measurements.* The stopped-flow measurements were carried out in a HI-Tech PQ/SF 53 sample handling unit. The volume of the observation cell is 40 $\mu$L. The Hi-Tech mixer is integrated into an On Line Intrument Systems spectrophotometer. The instrument is interfaced to an AST Premium 286 computer. Temperature was controlled by circulating water from a Lauda RMS-20 refrigerating bath around the drive syringes and the observation chamber.

*Binding of $BeF_3^-$ to Acto-S-1·ADP Complex.* The binding of $BeF_3^-$ was monitored by following the light scattering changes at 325 nm. Equal volumes (100 $\mu$L) of solutions containing actin, S-1, and $MgCl_2$ and ADP in 10 mM Tris and 10 mM KCl, pH 7.6, and $BeF_3^-$ diluted in the same buffer, were mixed in the stopped-flow unit. The final concentrations of the components were as follows: actin, 15 $\mu$M; S-1, 2.5 $\mu$M; $MgCl_2$, 2 mM; ADP, 1 mM; and $BeCl_2$ between 0 and 1.2 mM. NaF was kept constant at 5 mM. The drive pressure was 5 bar. Temperature was 22 °C.

*Dissociation of $\epsilon$ADP from the Acto-S-1·$\epsilon$ADP·$BeF_3^-$ Complex.* The dissociation was monitored via changes in the fluorescence of $\epsilon$ADP. The fluorophore $\epsilon$ADP was excited at 315 nm by a 75-W xenon arc lamp. The emitted light was detected after passage through a 1-mm thick WG360 optical filter. S-1 (5 $\mu$M) was preincubated with $MgCl_2$ (2 mM), $\epsilon$ADP (5 $\mu$M), $BeCl_2$ (500 $\mu$M), and NaF (5 mM) in 10 mM PIPES and 10 mM KCl, pH 7.0, for 30 min prior to the addition of 100 mM acrylamide. This solution was mixed in the stopped-flow unit with F-actin which contained 1 mM

ATP. The drive pressure was 5 bar. The temperature was 22 °C.

*Dissociation of εADP from the Actomyosin S-1·εADP·$AlF_4^-$ Complex.* The dissociation of εADP from the acto-S-1·εADP·$AlF_4^-$ complex was monitored by following the change in fluorescence of εADP in a Spex Fluorolog spectrophotometer at excitation and emission wavelengths 315 and 415 nm, respectively. S-1 (5 μM) was preincubated with $MgCl_2$ (2 mM), εADP (5 μM), $AlCl_3$ (4 mM), and NaF (16 mM) for 30 min at 22 °C. The standard solvent contained 10 mM PIPES and 100 mM KCl at pH 7.0. The fluorescence of εADP was measured in the presence of 100 mM acrylamide. Actin (from 3 to 40 μM) was added to the S-1 solution, and the change in fluorescence with time was monitored. The rate of εADP release was obtained by fitting the fluorescence decrease to eq 2.

*Analysis of Data.* In each experiment, at every concentration of beryllium fluoride or actin, 7–12 kinetic curves of 1000 points were stored and analyzed. The one- or two-exponential process with offset (eqs 1 and 2) was fitted to the data with the successive integration algorithm resident in the On Line Instrument System Software.

$$F = A \exp(-kt) + b \qquad (1)$$

$$F = A_1 \exp(-k_1 t) + A_2 \exp(-k_2 t) + b \qquad (2)$$

where $F$ is the light scattering or fluorescence signal in volts; $A$, $A_1$, and $A_2$ are the amplitudes of the signal change; $k$, $k_1$, and $k_2$ are the observed rate constants in seconds; $t$ is the time, and $b$ is the equilibrium signal (offset). Curves that differed in time constant or amplitude by more than two standard deviations from the mean were rejected. The concentration dependence of the time constants and the amplitudes was analyzed by the curve fitting program of the Sigma Plot Software, version 4.1.

*Note*: Even though the notation S-1·ADP·$BeF_3^-$ is adopted, it should be emphasized that this complex contains $Mg^{2+}$ and the correct structure is S-1·Mg·ADP·$BeF_3^-$.

## RESULTS

*Binding of Actin to S-1${}^{\neq}$·ADP·$BeF_3^-$.* The binding constants of actin to the S-1${}^{\neq}$·ADP·$BeF_3^-$ complex ($K_{actin}$) and the binding constant of $BeF_3^-$ to the acto-S-1·ADP complex ($K_{Be}$) were determined by the method used previously by Greene and Eisenberg in studies of the interactions of acto-S-1 with AMP-P(NH)P (1978) and with ADP, PPi (1980). The same method was also recently employed by Smith and Eisenberg (1990) to characterize the interactions of acto-S-1·ADP with vanadate. According to this method, the amount of actin bound to S-1·ADP at various $BeF_3^-$ concentrations was determined by centrifugation. At each $BeF_3^-$ concentration, an apparent binding constant ($K_{app}$) was obtained from the Scatchard plot relating the amount of bound S-1 to the amount of free S-1. Equation 3, which relates the apparent binding constant $K_{app}$ to 1/$BeF_3^-$, was derived according to Greene and Eisenberg (1978) with two additional approximations: the amount of free, uncomplexed S-1 and that of acto-S1 were considered to be negligible in the equilibrium system under study (actual calculations using known association constants showed that no more than 5% of total S-1 would exist in the S-1 form and less than 9% of the total acto-S-1 complexes would exist as acto-S-1).

$$K_{app} = \frac{1}{[BeF_3^-]}\frac{K_{actin}}{K_{Be}} + K_{actin} \qquad (3)$$

where $K_{actin}$ is the binding constants of actin to the S-1${}^{\neq}$·ADP·$BeF_3^-$ complex and $K_{Be}$ is the binding constant of $BeF_3^-$ to acto-S-1·ADP. Figure 1 shows the dependence of the apparent binding constants ($K_{app}$) on the inverse of $BeF_3^-$ concentration. The binding constant of actin to S-1${}^{\neq}$·ADP·$BeF_3^-$ obtained by linear extrapolation to inifinite $BeF_3^-$ concentration was 1.0 (±0.1) × $10^4$ $M^{-1}$, and the binding constant of $BeF_3^-$ to acto-S-1·ADP was 3.0 (±1.0) × $10^3$ $M^{-1}$. Very similar binding constants were also obtained for the respective interactions of actin, S-1·ADP, and vanadate (Smith & Eisenberg, 1990).

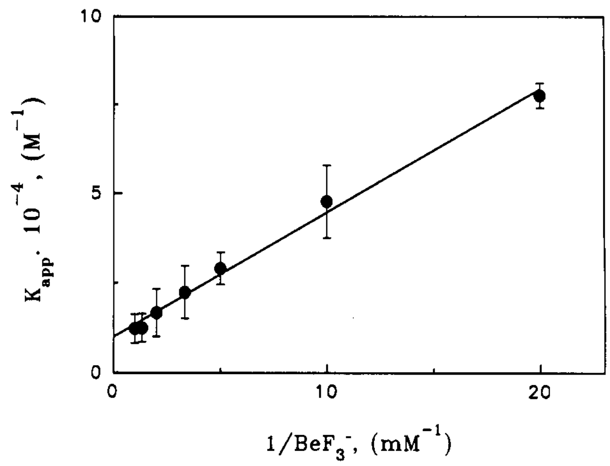


FIGURE 1: Apparent binding constants of actin to S-1·ADP as a function of beryllium fluoride conconcentration. The binding of actin to S-1·ADP was determined by ultracentrifugation of acto-S-1 solutions and the apparent binding constants were calculated as described under Materials and Methods. The actin concentration was 4 μM and S-1 concentrations varied between 0 and 10 μM. The concentrations of other components were 1 mM MgADP and $BeF_3^-$ as indicated. The standard solvent contained 40 mM NaCl and 10 mM Tris, pH 7.6. The *y* intercept, which corresponds to the binding constant of actin to S-1${}^{\neq}$·ADP·$BeF_3^-$, is 1.0 × $10^4$ (± 0.1) $M^{-1}$. The binding constant of $BeF_3^-$ to acto-S-1·ADP, derived from the slope of the straight line, is 3.0 × $10^3$ (± 1.0) $M^{-1}$. Each binding constant shown in this plot is the average of four separate binding determinations.

*Actin-Activated ATPase Activities of S-1 in the Presence of $BeF_3^-$.* $BeF_3^-$ has been shown to form a strongly bound ternary complex with S-1·ADP which significantly inhibits the S-1 ATPase (Phan & Reisler, 1992; Werber et al., 1992). The first set of experiments (Figure 1) revealed that actin binds only weakly to the ternary complex S-1${}^{\neq}$·ADP·$BeF_3^-$. To assess the effect of $BeF_3^-$ on the actin-activated ATPase activities of S-1, these activities were measured at various actin and $BeF_3^-$ concentrations under steady-state conditions. Figure 2 shows the double-reciprocal plots of the actin-activated ATPase of S-1·ADP in the presence of various $BeF_3^-$ concentrations. At low actin concentrations and at high $BeF_3^-$ concentrations, the inhibition of actin-activated ATPase by $BeF_3^-$ was significant. However, at high actin concentrations, there was very little inhibition of the acto-S-1 ATPase by $BeF_3^-$. Extrapolations of the experimental data to infinite actin concentration gave the same $V_{max}$ value (10 $s^{-1}$ ± 1.0) for all $BeF_3^-$ concentrations. The inhibitory constant, $K_i$, calculated from these activity measurements was 3.1 (±1.6) × $10^{-4}$ M, which agrees well with the $K_{Be}$ estimated from the equilibrium binding experiment (Figure 1).

It should be noted that although $BeF_3^-$ has recently been reported to perturb the structure of actin filaments (Orlova & Egelman, 1992), it appears to have little effect on the S-1 binding of actin and its S-1 ATPase activating function (Muhlrad et al., unpublished results).

*Dissociation of the Acto-S-1 Complexes as a Function of KCl Concentration.* A characteristic property of the

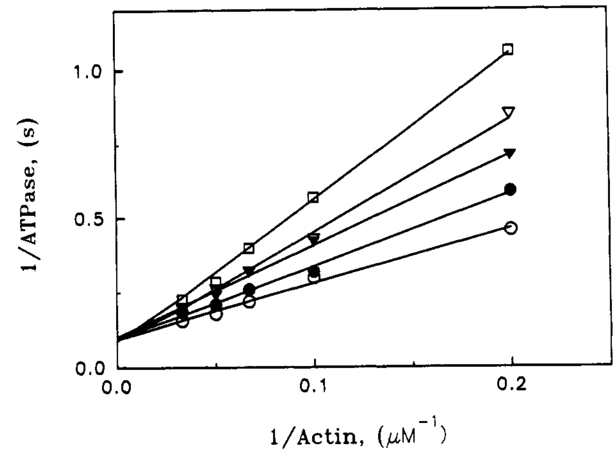


FIGURE 2: Double-reciprocal plots of the ATPase activity of acto-S-1 measured in the presence of beryllium fluoride. The specific acto-S-1 ATPase activities were measured by a colorimetric assay as described under Materials and Methods over the range of actin concentrations between 0 and 30 $\mu$M and beryllium fluoride concentrations of (○) 0, (●) 50 $\mu$M, (▼) 200 $\mu$M, (▽) 300 $\mu$M, and (□) 750 $\mu$M. All curves extrapolate to $V_{max}$ = 10 (± 1.0) $s^{-1}$.

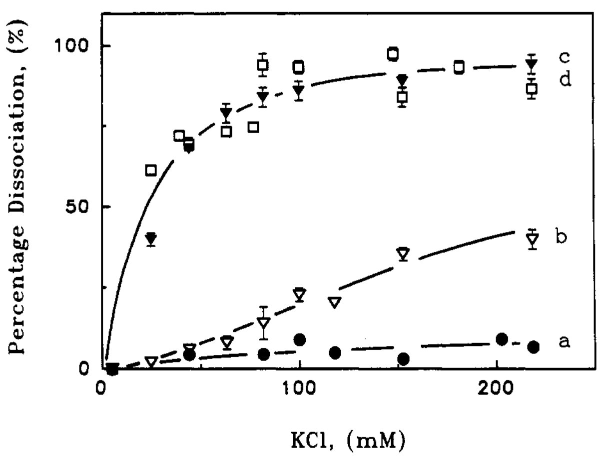


FIGURE 3: Dissociation of acto-S-1 nucleotide complexes as a function of KCl concentration. The dissociation of acto-S-1·nucleotide complexes was monitored by following light scattering changes at 325 nm as described under Materials and Methods. S-1 (2.5 $\mu$M) was mixed with actin (15 $\mu$M) in each experiment. The salt-dependence of dissociation of acto-S-1 was followed in the absence of nucleotide (curve a, ●) and in the presence of 1 mM MgADP (curve b, ▽), 2 mM MgATP$\gamma$S (curve d, □), and 1 mM MgADP and 500 $\mu$M $BeF_3^-$ (curve c, ▼).

AM**·ADP·$P_i$ intermediate and other weakly bound acto-myosin states is that their stability is highly salt-dependent (Highsmith, 1976; Chalovich et al., 1983). To determine whether the AM$^{\neq}$·ADP·$BeF_3^-$ complex exhibits the same property, the dissociation of the acto-S-1$^{\neq}$·ADP·$BeF_3^-$ complex was monitored as a function of salt concentration. Figure 3 relates the percentage of complex dissociation to KCl concentrations. In the absence of nucleotides (curve a), the dissociation of the acto-S-1 complex was very little affected by up to 200 mM KCl. In the presence of ADP (curve b), the salt dependence was stronger but not very significant, as at least 60–70% of the initial complex was still present at 200 mM KCl. On the other hand, the acto-S-1$^{\neq}$·ADP·$BeF_3^-$ interaction (curve c) was highly sensitive to salt, since more than 80% of the complex was dissociated at 100 mM KCl. Similar salt sensitivity was also observed for the weakly bound acto-S-1·ATP$\gamma$S complex (curve d), which is frequently used in lieu of acto-S-1·ATP (Buyer & Thomas, 1991). Also, a very similar salt-dependence of the acto-S-1·ATP interactions has been observed in earlier cosedimentation experiments (Chalovich et al., 1983; Chaussepied et al., 1988; Werber et al., 1992). These results suggest that the complex AS-1$^{\neq}$·ADP·$BeF_3^-$ resembles the intermediate states AS-1**·ADP·$P_i$.

*Rate of Binding of $BeF_3^-$ to the Acto-S-1·ADP Complex.* The rate of $BeF_3^-$ binding to acto-S-1·ADP complex was determined by following the time course of light scattering decrease at 325 nm in the stopped-flow apparatus. The decrease in light scattering occurred as the acto-S-1·ADP·$BeF_3^-$ complex formed and then rapidly dissociated to actin and S-1·ADP·$BeF_3^-$. Figure 4A (upper curve) shows the time course of light scattering decrease at 50 $\mu$M $BeF_3^-$. The observed rate constant ($k_{obs}$) and the amplitude of the decrease

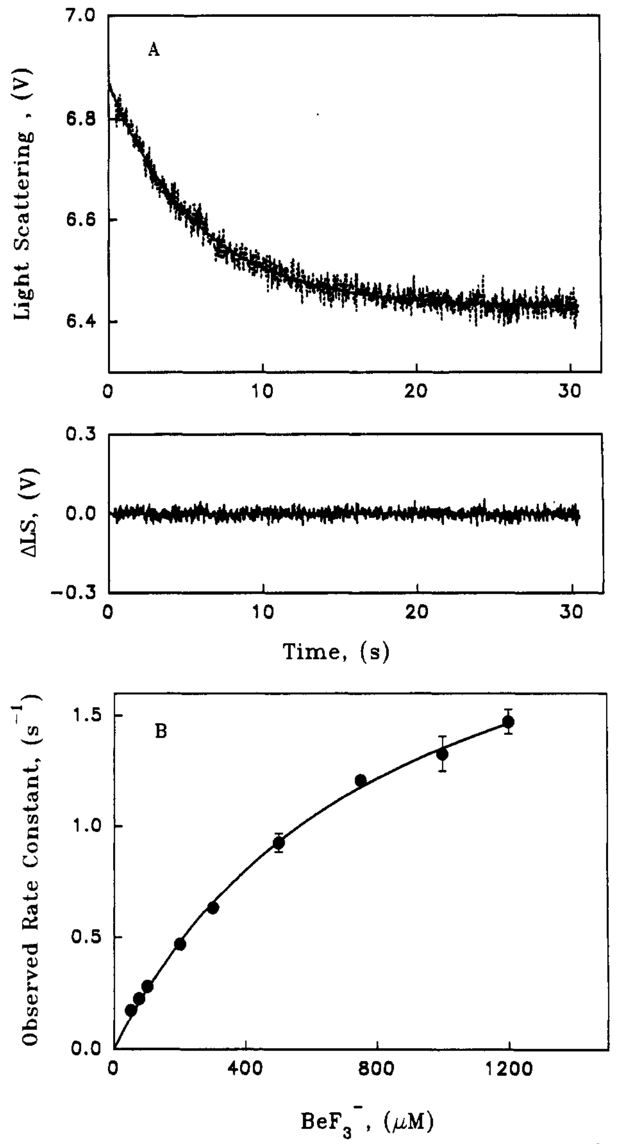


FIGURE 4: Rate of light scattering changes observed on binding $BeF_3^-$ to acto-S-1·ADP. The rate of $BeF_3^-$ binding to acto-S-1 ADP was determined by mixing $BeF_3^-$ with acto-S-1·ADP and monitoring the decrease in light scattering at 325 nm in a stopped-flow apparatus. The scattering decrease at each $BeF_3^-$ concentration, corresponding to the dissociation of acto-S-1·ADP·$BeF_3^-$, fitted a single exponential term. (A) Upper curve, light-scattering signal for the binding of 50 $\mu$M $BeF_3^-$ to acto-S-1·ADP; the smooth curve drawn through the experimental trace is the computer fit to a single-exponential equation; $k_{obs}$ = 0.17 (± 0.08) $s^{-1}$. Lower curve, the residual plot generated from the computer fit. (B) Dependence of the $k_{obs}$ on $BeF_3^-$ concentration. Values for $k_{obs}$ in the range between 0 and 1.2 mM $BeF_3^-$ were fitted to a hyperbola with a maximum rate of 2.5 (± 0.5) $s^{-1}$ and an apparent binding constant of 1.2 × $10^3$ (± 0.2) $M^{-1}$. Experimental conditions were as described under Materials and Methods. The voltage change ($V$) was proportional to the change in light scattering intensity.

Scheme I

$$A{\cdot}S\text{-}1{\cdot}ADP + BeF_3^- \underset{}{\overset{K'_1}{\rightleftharpoons}} (A{\cdot}S\text{-}1{\cdot}ADP{\cdot}BeF_3) \overset{K'_2}{\rightleftharpoons}$$
$$A{\cdot}S\text{-}1^{\neq}{\cdot}ADP{\cdot}BeF_3^- \longrightarrow A + S\text{-}1^{\neq}{\cdot}ADP{\cdot}BeF_3^-$$

were obtained by fitting the scattering change to a single exponential term (solid curve drawn through the experimental trace). The residual plot of the fit is shown in the lower panel of Figure 4A. Figure 4B shows the values of $k_{obs}$ as a function of $BeF_3^-$ concentration. The data were fitted to a hyperbola (solid line drawn through data points) which corresponds to a maximum rate of $BeF_3^-$ binding of 2.5 (± 0.5) $s^{-1}$ and an apparent binding constant of 1.2 (± 0.2) × $10^3$ $M^{-1}$. These results suggest that the binding of $BeF_3^-$ to acto-S-1·ADP consists of at least two steps. The simplest scheme consistent with the kinetic data is shown in Scheme I, where $K'_1$ is the equilibrium constant for the formation of the collisional complex and $K'_2$ the isomerization constant of the collisional complex to the AS-1$^{\neq}$·ADP·$BeF_3^-$ complex which then rapidly dissociates into actin and S-1$^{\neq}$·ADP·$BeF_3^-$. Scheme I, however, as shown below, can not account for the data obtained from studies on the interactions of actin with S-1·εADP·$BeF_3^-$ (Figure 5). Therefore, an alternative scheme will be adopted and analyzed in the Discussion.

It should be noted that the apparent binding constant obtained in this experiment (Figure 4) and the one obtained from equilibrium binding (Figure 1) are not comparable. In Figure 1, the apparent binding constant of $BeF_3^-$ to acto-S-1·ADP was estimated at infinite actin concentration and in the presence of 40 mM NaCl and 10 mM Tris, while in Figure 4, the apparent binding constant was obtained at 15 μM actin and in the presence of 10 mM KCl and 10 mM Tris.

*Rate of Dissociation of $BeF_3^-$ from the Acto-S-1·εADP·$BeF_3^-$ Complex.* The rate of dissociation of $BeF_3^-$ from the acto-S-1·εADP $BeF_3^-$ complex was studied by monitoring the time course of the εADP fluorescence decrease, as bound εADP was displaced by actin and quenched by acrylamide. The rationale for this experiment relies on the preferential quenching of the free εADP by acrylamide (Ando et al., 1982). The fluorescence intensity of εADP bound to S-1 is high, but when the analog is displaced from S-1 by actin and released into the medium, its fluorescence decreases within mixing time due to acrylamide quenching (Ando et al., 1982). Even though the release of εADP is monitored in this experiment, the rate-limiting step is the dissociation of $BeF_3^-$; therefore, the rate of εADP release reflects the dissociation of $BeF_3^-$ from the acto-S-1·εADP·$BeF_3^-$ complex. In these experiments, a solution of S-1·εADP·$BeF_3^-$ was mixed with an actin solution containing a large excess of ATP. The presence of ATP ensures that the dissociation step of εADP is irreversible (Rosenfeld & Taylor, 1987).

Figure 5A (upper panel) shows the dissociation of εADP induced by 10 μM actin. The fluorescence decrease fitted two exponential terms (solid curve drawn through the experimental trace). The residual plot of the two-exponential fit is shown in the lower panel of Figure 5A. The biexponential release of εADP was not related to isozyme composition of S-1; similar rates were observed with either S-1(A1) or S-1(A2). The simplest kinetic scheme which is consistent with earlier results on the interactions of S-1·ADP with $BeF_3^-$ (Phan & Reisler, 1992) and also accounts for two exponential terms is described in Scheme II, where S-1$^{\neq}$·εADP·$BeF_3^-$ and S-1$^{\neq\neq}$·εADP·$BeF_3^-$ represent two different isomerized states which have been defined in earlier work (Phan & Reisler, 1992). The isomerization rate of the complex S-1$^{\neq}$·

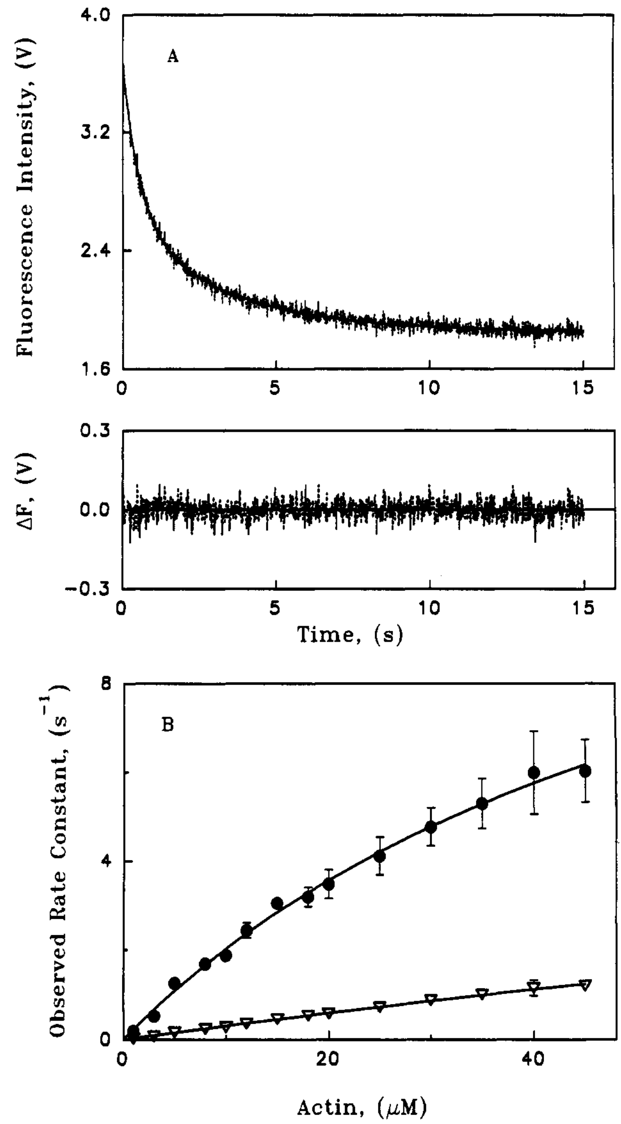


FIGURE 5: Rate of $BeF_3^-$ dissociation from the acto-S-1·εADP·$BeF_3^-$ complex. The rate of dissociation of $BeF_3^-$ was measured by adding 0–45 μM (final) actin to the S-1·εADP·$BeF_3^-$ complex in the presence of 100 mM acrylamide and 1 mM MgATP in a stopped-flow apparatus. The fluorescence decrease at each actin concentration fitted two exponential terms. (A) Upper curve, the fluorescence decrease due to the dissociation of εADP from the actomyosin S-1εADP·$BeF_3^-$ complex at 10 μM actin; the smooth curve drawn through the experimental trace is the computer fit to two exponential terms; the observed rate constants are 1.80 (± 0.07) $s^{-1}$ and 0.30 (± 0.01) $s^{-1}$. Lower curve, the residual plot generated from the computer fit. (B) Dependence of the rate constants on actin concentration. The two apparent rate constants were plotted as a function of actin concentration. Values of the observed rates for the range of actin concentrations between 0 and 45 μM were fitted to a hyperbola drawn through the data points. The process with the larger rate constant had a maximum rate constant of 15 (± 1.2) $s^{-1}$ and an apparent binding constant of 1.6 × $10^4$ (± 0.2) $M^{-1}$. An accurate determination for the maximum rate of the slower process could not be made; it must have been at least 1.3 $s^{-1}$. Experimental conditions were as described under Materials and Methods. The voltage change (*V*) was proportional to the change in fluorescence.

εADP·$BeF_3^-$ to the complex S-1$^{\neq\neq}$·εADP·$BeF_3^-$ was determined to be between $10^{-6}$ and $10^{-4}$ $s^{-1}$ (Phan & Reisler, 1992). In that study, this isomerization step was thought to be virtually irreversible, and hence the notation S-1$^{i}$·εADP·$BeF_3^-$ was adopted. However, since actin induces a complete dissociation of εADP and $BeF_3^-$ from the S-1$^{i}$·εADP·$BeF_3^-$ complex (data not shown), its notation was changed to S-1$^{\neq\neq}$·εADP·$BeF_3^-$. The distribution of the two complexes S-1$^{\neq}$·εADP·$BeF_3^-$ and

Scheme II

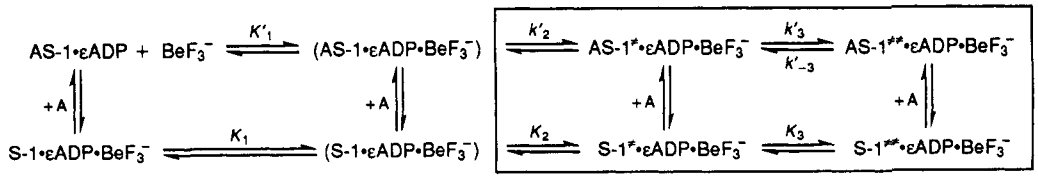

$S\text{-}1^{\neq\neq}\cdot\epsilon ADP\cdot BeF_3^-$ depends on the preincubation time of S-1, $\epsilon$ADP, and $BeF_3^-$ (Phan & Reisler, 1992). The longer the preincubation time, up to at least 45 min, the greater the $S\text{-}1^{\neq\neq}\cdot\epsilon ADP\cdot BeF_3^-$ population. However, after approximately 45 min, the system reached an equilibrium with about equal amounts (50:50) of the two complexes present (data not shown).

When the $S\text{-}1\cdot\epsilon ADP\cdot BeF_3^-$ solution is mixed with actin, in the presence of a large excess of ATP (the boxed part of Scheme II), the dissociation of $\epsilon$ADP is practically irreversible (Rosenfeld & Taylor, 1987). Also, the rate of dissociation of $\epsilon$ADP is much faster (Rosenfeld & Taylor, 1987) than the rate of release of $BeF_3^-$; therefore, step 2′ is also irreversible. According to Scheme II, the two rate constants obtained experimentally correspond to $k'_{-2}$ and $k'_{-3}$, unless $BeF_3^-$ is released through alternative pathways. Figure 5B shows the dependence of the observed rate constants on actin concentrations. The data were fitted to a hyperbola (solid lines drawn through the data points). This hyperbolic dependence is consistent with a rate-limiting isomerization step on the $\epsilon$ADP dissociation pathway. The process with the larger rate constant had a maximum rate constant of 15 ($\pm$ 1.2) $s^{-1}$ and an apparent binding constant of 1.6 ($\pm$ 0.2) $\times 10^4$ $M^{-1}$. Due to experimental limitations, the maximum rate for the second process could not be determined, but it must have been at least 1.3 $s^{-1}$ (Figure 5).

In order to determine which steps correspond to the larger rate constant, the distribution of the amplitudes $A_1$ and $A_2$ was analyzed. The ratio of two amplitudes did not show any dependence on actin concentration (data not shown). This lack of actin dependence of the two amplitudes is consistent with Scheme II. Since the rate constant of isomerization between the $S\text{-}1^{\neq}\cdot\epsilon ADP\cdot BeF_3^-$ and $S\text{-}1^{\neq\neq}\cdot\epsilon ADP\cdot BeF_3^-$ complexes was approximately $10^{-4}$ $s^{-1}$ (under the experimental conditions used), these complexes interacted with actin as two independent populations. According to the proposed scheme, the distribution of the amplitudes $A_1$ and $A_2$ depends on $K_3$, which determines the fractions of $S\text{-}1^{\neq}\cdot\epsilon ADP\cdot BeF_3^-$ and $S\text{-}1^{\neq\neq}\cdot\epsilon ADP\cdot BeF_3^-$ present at the time of mixing with actin. Under the experimental conditions used, regardless of the actin concentration, the ratio of the two amplitudes $A_1$ and $A_2$ was 60% and 40%, respectively. It has been observed that the contribution of the process with the smaller rate constant ($A_2$) increased as the preincubation time was increased (data not shown). These results suggest that the faster process corresponds to the dissociation of $BeF_3^-$ from the $A\cdot S\text{-}1^{\neq}\cdot\epsilon ADP\cdot BeF_3^-$ complex ($k'_{-2}$), and the slower process corresponds to the release of $BeF_3^-$ from the more stable isomerized $AS\text{-}1^{\neq\neq}\cdot\epsilon ADP\cdot BeF_3^-$ complex either by isomerizing to the $A\cdot S\text{-}1^{\neq}\cdot\epsilon ADP\cdot BeF_3^-$ complex ($k'_{-3}$) or directly to A·S-1·$\epsilon$ADP.

*Dissociation of $AlF_4^-$ from the Acto-S-1·$\epsilon$ADP·$AlF_4^-$ Complex.* The kinetic results presented above and most of all the fast dissociation of $BeF_3^-$ from the acto-$S\text{-}1^{\neq}\cdot\epsilon ADP\cdot BeF_3^-$ complex lead to certain predictions about the effect of $BeF_3^-$ on muscle fiber mechanics. It may be expected that $BeF_3^-$ will not inhibit the recovery of force in skinned muscle fibers. In fact, it has been observed that $BeF_3^-$, while suppressing force development in skinned muscle fibers under isometric conditions, had only a small effect on force recovery (force recovery was estimated to be at most 3-fold slower than in a normal activation; P. B. Chase, personal communication). On the other hand, aluminum fluoride, an analog of beryllium fluoride, strongly inhibited force recovery in skinned muscle fibers (Chase & Kushmerick, 1993). The half-time ($t_{1/2}$) for force recovery in aluminum-treated fibers was 2–4 min, which was many fold slower than the force recovery from $BeF_3^-$. In an attempt to understand this difference, the dissociation of $AlF_4^-$ from the complex acto-$S\text{-}1^{\neq}\cdot\epsilon ADP\cdot AlF_4^-$ in solution was examined. Figure 6 shows the time course of the fluorescence decrease of $\epsilon$ADP at 8 $\mu$M actin in 100 mM KCl and 10 mM PIPES, pH 7.0. The high ionic strength was chosen to simulate the conditions used in fiber experiments. The fluorescence decrease fitted two exponential terms (curve drawn through the experimental trace). The observed rate constants at 8 $\mu$M actin were $1.4 \times 10^{-3}$ ($\pm$ $1.0 \times 10^{-5}$) $s^{-1}$ and $1.9 \times 10^{-4}$ ($\pm$ $5.0 \times 10^{-6}$) $s^{-1}$. By analogy to the analysis of the $BeF_3^-$ system, the two rate constants were attributed to the dissociation of $AlF_4^-$ from the two complexes $AS\text{-}1^{\neq}\cdot\epsilon ADP\cdot AlF_4^-$ and $AS\text{-}1^{\neq\neq}\cdot\epsilon ADP\cdot AlF_4^-$. These two rate constants were about 10–30-fold smaller than the corresponding rate constants obtained for the dissociation of $BeF_3^-$ from the acto-S-1·$\epsilon$ADP·$BeF_3^-$ complex under the same conditions (data not shown). Thus, as noted by Werber et al. (1992), actin displaces $AlF_4^-$ much slower than it displaces $BeF_3^-$. This observation is consistent with the faster recovery of actin-activated S-1 ATPase from $BeF_3^-$ inhibition than $AlF_4^-$ inhibition; even though, in the absence of actin, the $S\text{-}1^{\neq}\cdot ADP\cdot BeF_3^-$ complex is much more stable than the $S\text{-}1^{\neq}\cdot ADP\cdot AlF_4^-$ complex (Werber et al., 1992). The difference in the rates of dissociation of $AlF_4^-$ and $BeF_3^-$ from

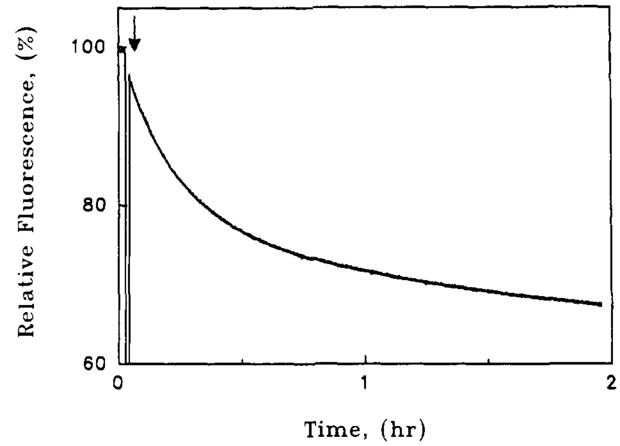


FIGURE 6: Dissociation of $AlF_4^-$ from the acto-S-1·$\epsilon$ADP·$AlF_4^-$ complex. S-1 (5 $\mu$M) was preincubated with $MgCl_2$ (2 mM), $\epsilon$ADP (5 $\mu$M) and $AlF_4^-$ in 100 mM KCl and 10 mM PIPES, pH 7.0. At the time indicated by the arrow, actin (8 $\mu$M) was added to the solution. Fluorescence intensities were measured in the presence of acrylamide (100 mM). The fluorescence decrease fitted two exponential terms (the smooth curve drawn over the experimental trace). The observed rate constants were $1.4 \times 10^{-3}$ ($\pm$ $1.0 \times 10^{-5}$) $s^{-1}$ and $1.9 \times 10^{-4}$ ($\pm$ $5.0 \times 10^{-6}$) $s^{-1}$.

Scheme III

$$\text{AS-1·ADP} + \text{BeF}_3^- \xrightleftharpoons{K'_1} (\text{AS-1·ADP·BeF}_3^-) \xrightleftharpoons{K'_2} \text{AS-1}^{\neq}\text{·ADP·BeF}_3^- \xrightleftharpoons{K'_3} \text{AS-1}^{\neq\neq}\text{·ADP·BeF}_3^-$$

acto-S-1 complexes can account, at least qualitatively, for the difference in the rates of force recovery observed in fibers.

## DISCUSSION

In this study, we examined the interactions of BeF$_3^-$ with actomyosin. Our goal was to derive a kinetic description of these interactions and to further test the hypothesis that the S-1$^{\neq}$·ADP·BeF$_3^-$ complex is an analog of the S-1$^{**}$·ADP·P$_i$ state. Several well-defined requirements have to be satisfied by such an analog in the presence of actin. These include weak binding to actin, acceleration of product release by actin, and strong dependence of complex stability on ionic strength. Our results show that the ternary complex S-1$^{\neq}$·ADP·BeF$_3^-$ binds weakly to actin. The week binding of S-1$^{\neq}$·ADP·BeF$_3^-$ to actin resembles that of the S-1$^{**}$·ADP·P$_i$ state (White & Taylor, 1976; Stein et al., 1979). Furthermore, just as P$_i$ binds weakly to the actomyosin·ADP complex (White & Taylor, 1976), BeF$_3^-$, which binds to the S-1·ADP complex with high affinity ($K_a = 5 \times 10^5$ M$^{-1}$) (Phan & Reisler, 1992), has a much lower affinity for the acto-S-1·ADP complex (Figure 1).

As shown in Scheme I, the binding of BeF$_3^-$ to the acto-S-1·ADP complex proceeds in at least two steps: a rapid and weak binding of BeF$_3^-$ to acto-S-1·ADP complex to form a collisional intermediate AS-1·ADP·BeF$_3^-$, followed by a slower conformational change to the isomerized AS-1$^{\neq}$·ADP·BeF$_3^-$ complex. According to the description of the results shown in Figure 4 by Scheme I, the maximum observed binding rate constant (2.5 ± 0.5 s$^{-1}$) should correspond to the rate-limiting step ($k'_2 + k'_{-2}$). However, the value of $k'_{-2}$ (15 ± 1.2 s$^{-1}$) determined from the dissociation experiment (Figure 5) was much larger than the maximum observed binding rate. This discrepancy between the two rate constants rules out Scheme I as a possible model to describe the interactions of BeF$_3^-$ with acto-S-1·ADP. A more comprehensive scheme which can also account for the two rates associated with the release of BeF$_3^-$, and in which a third step that describes the isomerization of AS-1$^{\neq}$·ADP·BeF$_3^-$ to AS-1$^{\neq\neq}$·ADP·BeF$_3^-$ is included, is shown in Scheme III, where $K'_1$ is the equilibrium constant for the formation of the collisional complex, $K'_2$ the isomerization constant of the collisional complex to the AS-1$^{\neq}$·ADP·BeF$_3^-$ complex, and $K'_3$ the isomerization constant of AS-1$^{\neq}$·ADP·BeF$_3^-$ to AS-1$^{\neq\neq}$·ADP·BeF$_3^-$.

Scheme III represents a special case of a general system, A + B ↔ C ↔ D ↔ E + F, which has been described by Bernasconi (1976). In principle, three time constants corresponding to the three transitions should be observed. However, only one time constant, assigned to the isomerization of AS-1$^{\neq}$·ADP·BeF$_3^-$ to AS-1$^{\neq\neq}$·ADP·BeF$_3^-$, was observed in this case. Indeed, the first two reactions, the formation of the collisional complex (AS-1·ADP·BeF$_3^-$) and the isomerization of this complex to AS-1$^{\neq}$·ADP·BeF$_3^-$, would be too fast to be measured (see Appendix for expressions of time constants). In line with this, the amplitudes of the scattered light show that a considerable fraction of acto-S-1 complex was rapidly dissociated by BeF$_3^-$ prior to the kinetically observed transition. The observed rate constant (2.5 ± 0.5 s$^{-1}$), to a good approximation (see Appendix), corresponds to $k'_3$. Thus, $K'_3$ can be estimated to be at most 2.

In the absence of actin, the rate of dissociation of BeF$_3^-$ and εADP from the S-1$^{\neq}$·εADP·BeF$_3^-$ complex is ~10$^{-4}$ s$^{-1}$ (Phan & Reisler, 1992). This rate is activated at least 10$^4$-fold by actin. Similar actin-activated ligand release has also been observed for the dissociation of vanadate from the S-1$^{\dagger}$·ADP·V$_i$ complex (Goodno & Taylor, 1982). The actin-activated ligand release provides additional evidence for the hypothesis that the AS-1$^{\neq}$·ADP·BeF$_3^-$ resembles the AS-1$^{**}$·ADP·P$_i$ intermediate. It should be noted that the rate of dissociation of BeF$_3^-$ from the complex AS-1$^{\neq}$·ADP·BeF$_3^-$ calculated in this work is much faster than the rate of decomposition of the AS1$^{\neq}$·ADP·BeF$_3^-$ complex estimated by Werber et al. (1992). However, their ATPase measurements did not have sufficient time resolution to detect the fast dissociation of BeF$_3^-$.

Finally, another property that the AS-1$^{\neq}$·ADP·BeF$_3^-$ complex shared with the transition state AM$^{**}$·ADP·P$_i$ is the dependence of their stability on ionic strength. Overall, these results strongly suggest that the AM$^{\neq}$·ADP·BeF$_3^-$ is an analog of the AM$^{**}$·ADP·P$_i$ intermediate state.

Our results show that actin accelerates the release of ligands BeF$_3^-$ and ADP and that BeF$_3^-$ does not inhibit actomyosin ATPase at high actin concentrations. The fast dissociation of BeF$_3^-$ from the complex AM$^{\neq}$·ADPBeF$_3^-$ observed in this work is consistent with the finding that BeF$_3^-$ has only a small effect on force recovery in skinned muscle fibers (P. B. Chase, personal communication). BeF$_3^-$, AlF$_4^-$, and V$_i$, however, strongly inhibited force development by skinned muscle fibers under isometric conditions (Dantzig & Goldman, 1985; Chase & Kushmerick, 1993). In order to reconcile the lack of significant inhibition of actomyosin ATPase by these analogs with the inhibition of isometric force development in muscle fibers, it has been proposed that the rate-limiting step in ATPase cycle was different from that of the cross-bridge cycle (Goldman, 1987). Also, several other factors could contribute to kinetic differences between solution and fiber work. First, the ionic strength in most fiber experiments is at least 10–100-fold higher than the ionic strength adopted in solution work. Under higher ionic strength conditions, the rate of release of product is slowed dramatically (Phan and Reisler, unpublished data). Second, the lower temperature (10–12 °C) used in fiber experiments may also contribute to kinetic differences with solution studies. Finally, strained cross-bridges appear to have higher affinity for phosphate and its analogs, thus affecting force development and recovery (Hibberd & Trentham, 1986). This may further complicate direct comparison of solution and fiber experiments.

The results obtained in this work strongly suggest an analogy between the AM$^{\neq}$·ADP·BeF$_3^-$ complex and the intermediate state AM$^{**}$·ADP·P$_i$. Similarity between this intermediate state and the complex formed from actin, S-1, ADP and vanadate has also been inferred (Goodno & Taylor, 1982, Smith & Eisenberg, 1991). However, the absorption of vanadate in the UV region, which excludes the use of some spectroscopic methods, and its tendency to polymerize greatly limit the detailed kinetic characterization of actin interaction with the complex M$^{\dagger}$·ADP·V$_i$. The S-1$^{\neq}$·ADP·AlF$_4^-$ complex has also been compared to the S-1$^{**}$·ADP·P$_i$ state (Werber et al., 1992). However, some caution is called for in the interpretations of experiments on the AlF$_4^-$ complexes with S-1·ADP. The unusual biphasic dependence of the observed rates of formation of S-1$^{\neq}$·ADP·AlF$_4^-$ on AlCl$_3$ concentration (Werber et al., 1992) and at least a 10-fold lower activation of AlF$_4^-$ release from S-1 than that of BeF$_3^-$ and V$_i$ (Werber et al., 1992) point to some differences between these complexes with the S-1$^{\neq}$·ADP·AlF$_4^-$ complex. Therefore, BeF$_3^-$, which is spectroscopically silent, does not polymerize, and its interactions with S-1 and acto-S-1 are amenable to kinetic analysis, appears to be an analog of choice for the characterization of the intermediates associated with the $Mg^{2+}$-dependent ATPase pathway.

After completion of this work, four forms of beryllium fluoride complexes with S-1 have been reported in abstract form (Henry et al., 1993). It is conceivable that the isomerized states of S-1·ADP·$BeF_3^-$ correspond to the different forms of beryllium fluoride complexes.

## ACKNOWLEDGMENT

We thank Dr. Bryant Chase for sharing with us his unpublished data, Drs. Joseph Chalovich and Andras Muhlrad for helpful discussion of the manuscript, Dr. Earl Homsher for assistance with the fiber experiments, and Dr. Shwu-Hwa Lin for her help with the stopped-flow experiments.

## APPENDIX

*Analysis of Scheme III.* Although in general three time constants corresponding to the three transition should be observed, the first reaction, formation of the collisional complex (AS-1·ADP·$BeF_3^-$), is unobservable.

The expression for the time constant of the second reaction, the isomerization of collisional complex to the AS-$1^{\neq}$·ADP·$BeF_3^-$ complex, was adopted from Bernasconi (1976). The concentration of the acto-S-1·ADP was omitted as being negligible compared to $[BeF_3^-]$ (pseudo-first-order conditions)

$$\text{time constant} = k'_2 \frac{K'_1[\mathrm{BeF_3^-}]}{1 + K'_1[\mathrm{BeF_3^-}]} + k'_{-2} \quad (1)$$

where $[BeF_3^-]$ represents the equilibrium concentration of $BeF_3^-$. By using the value of 15 $s^{-1}$ for $k'_{-2}$, 50 $\mu$M for $[BeF_3^-]$ and $10^3$ $M^{-1}$ as an upper limit for $K'_1$ (it cannot be much larger than the apparent binding constant obtained from Figure 4, which, to a good approximation, corresponds to the product of $K'_1$ and $K'_2$); and assuming that $k'_2$ should be greater than $k'_{-2}$, the time constant can be estimated to be at least 300 $s^{-1}$, which is too fast for detection in our system.

The expression for the time constant of the third reaction, the isomerization of the AS-$1^{\neq}$·ADP·$BeF_3^-$ complex to the AS-$1^{\neq\neq}$·ADP·$BeF_3^-$ complex, is given in eq 2 [adapted from Bernasconi (1976)], omitting again the concentration of acto-S-1·ADP.

$$\text{time constant} = k'_3 \frac{K'_1[\mathrm{BeF_3^-}]K'_2}{1 + K'_1[\mathrm{BeF_3^-}] + K'_1[\mathrm{BeF_3^-}]K'_2} + k'_{-3}[\mathrm{AS\text{-}1^{\neq\neq}\cdot ADP\cdot BeF_3^-}] \quad (2)$$

Using the value of $10^3$ $M^{-1}$ for $K'_1$ and approximating the equilibrium concentrations of the reactants by their initial concentrations, eq 2 can be simplified to

$$\text{time constant} = k'_3 \frac{0.05K'_2}{1 + 0.05 + 0.05K'_2} + k'_{-3}(2.5 \times 10^{-6}\ \mathrm{M}) \quad (3)$$

Even though the value of $K'_2$ is unknown, inspection of eq 3 would justify the approximation of the observed binding rate constant to $k'_3$. It is noted again that although the experimentally measured decrease in light scattering reflects the dissociation of the AS-$1^{\neq\neq}$·ADP·$BeF_3^-$ complex to actin and S-$1^{\neq\neq}$·ADP·$BeF_3^-$, this process is fast, and therefore the observed rate corresponds to $k'_3$. The value of $K'_3$ can be estimated to be at most 2 (taking the minimum value of 1.3 $s^{-1}$ for $k'_{-3}$).

## REFERENCES

Ando, T., Duke, A. J., Tonomura, Y., & Morales, A. F. (1982) *Biochem. Biophys. Res. Commun. 109*, 1–6.
Bagshaw, C. R., & Trentham, D. R. (1974) *Biochem. J. 141*, 331–349.
Beck, T. W., Chase, P. B., & Kushmerick, M. J. (1992) *Biophys. J. 61*, A435.
Bernasconi, C. F. (1976) *Relaxation Kinetics*, p 42, Academic Press, New York.
Buyer, C. L., & Thomas, D. D. (1991) *Biochemistry 30*, 11036–11045.
Chalovich, J. M., Greene, L. E., & Eisenberg, E. (1983) *Proc. Natl. Acad. Sci. U.S.A 80*, 4909–4913.
Chase, B. P., & Kushmerick, M. J. (1993) *J. Physiol. 460*, 231–246.
Chaussepied, P., Morales, M. F., & Kassab, R. (1988) *Biochemistry 27*, 1778–1785.
Combeau, C., & Carlier, M. F. (1988) *J. Biol. Chem. 263*, 17429–17436.
Dantzig, J. A., & Goldman, Y. E. (1985) *J. Gen. Physiol. 86*, 305–327.
Godfrey, J. E., & Harrington, W. F. (1970) *Biochemistry 9*, 886–895.
Goldman, Y. E. (1987) *Annu. Rev. Physiol. 49*, 637–654.
Goodno, C. C. (1979) *Proc. Natl. Acad. Sci. U.S.A. 76*, 2620–2624.
Goodno, C. C., & Taylor, E. W. (1982) *Proc. Natl. Acad. Sci. U.S.A. 79*, 21–25.
Goody, R. S., Hofmann, W., Reedy, M. K., Magid, A., & Goodno, C. C. (1980) *J. Muscle Res. Cell Motil. 1*, 198–199.
Greene, L. E., & Eisenberg, E. (1978) *Proc. Natl. Acad. Sci. U.S.A. 75*, 54–58.
Greene, L. E., & Eisenberg, E. (1980) *J. Biol. Chem. 255*, 549–554.
Henry, G. D., Maruta, S., Sykes, B. D., & Ikebe, M. (1993) *Biophys. J. 64*, A141.
Hibberd, M. G., & Trentham, D. R. (1986) *Annu. Rev. Biophys. Biophys. Chem. 15*, 119–161.
Highsmith, S. (1976) *J. Biol. Chem. 251*, 6170–6172.
Issartel, J. P., Dupuis, A., Lunardi, J., & Vignais, P. V. (1991) *Biochemistry 30*, 4726–4733.
Laemmli, U. K. (1970) *Nature 227*, 680–685.
Lymn, R. W., & Taylor, E. W. (1970) *Biochemistry 9*, 2975–2983.
Lymn, R. W., & Taylor, E. W. (1971) *Biochemistry 10*, 4617–4624.
Maruta, S., Henry, G. D., Sykes, B. D., & Ikebe, M. (1991) *Biophys. J. 59*, 436a.
Orlova, A., & Egelman, E. H. (1992) *J. Mol. Biol. 227*, 1043–1053.
Phan, B. C., & Reisler, E. (1992) *Biochemistry 31*, 4787–4793.
Robinson, J. D., Davis, R. L., & Steinberg, M. (1986) *J. Bioenerg. Biomembr. 18*, 521–531.
Rosenfeld, S. S., & Taylor, E. W. (1987) *J. Biol. Chem. 262*, 9994–9999.
Smith, S. J., & Eisenberg, E. (1990) *Eur. J. Chem. 193*, 69–73.
Spudich, J. A., & Watt, S. (1971) *J. Biol. Chem. 246*, 4866–4871.
Stein, L. A., Schwarz, R., Chock, P. B., & Eisenberg, E. (1979) *Biochemistry 18*, 3895–3909.
Weeds, A. S., & Pope, B. (1977) *J. Mol. Biol. 111*, 129–157.
Wells, C., & Bagshaw, C. R. (1984) *J. Muscle Res. Cell Motil. 5*, 97–112.
Werber, M. M., Peyser, Y. M., & Muhlrad, A. (1992) *Biochemistry 31*, 7190–7197.
White, H. D., & Taylor, E. W. (1976) *Biochemistry 15*, 5818–5826.